

## Analysis of the coordination geometry in copper complexes

C RAMAKRISHNAN\* and Y S GEETHA†

Molecular Biophysics Unit, Indian Institute of Science, Bangalore 560012, India

† Present address: Protein Identification Resource, National Biomedical Research Foundation, Georgetown University Medical Center, Washington DC 20007, USA

MS received 4 October 1989; revised 3 March 1990

**Abstract.** Geometrical parameters associated with a metal coordinated system have been analysed using data from 75 structures of copper complexes involving 370 coordination bonds. Coordination bond length and coordination bond angle, and deviation of the metal atom from the plane of equatorial ligand atoms have been analysed in detail for both oxygen and nitrogen ligand atoms. At the ligand end, the parameters defined closely follow that of the hydrogen bonded system and are related to the lone pair orbital directions. We find that (1) for oxygen ligands, the axial bond lengths are distinctly longer than the equatorial ones in octahedral (OCT) and square pyramidal (PY) geometries. The situation is reversed for trigonal bi-pyramidal (TBP) geometry with nitrogen ligands. (2) The coordination bond angle involving axial atoms varies between 130 and 180° for the OCT case and 170 and 180° for TBP geometry. Angles lying around 90° range from 75–105° with a few exceptions in OCT geometry. (3) The metal atom lies very nearly in the equatorial plane in TBP, while it deviates significantly in others. The extent of deviation can be explained qualitatively with the pull of the metal atom by the axial atoms. (4) The distribution of the ligand end parameters indicate that the bond direction strongly tends to cling to the associated orbital. When the ligand atom has two orbitals, the influence of the non-associated orbital is not significant and is far less as compared to hydrogen bonding.

**Keywords.** Copper coordination; coordination geometry; data analysis.

### 1. Introduction

The importance of metal ions in biological systems is quite well known. One of the very interesting features of a metal coordinated system is the concerted spatial arrangement of the ligands around the metal ion. In this paper, the crystal structure data on a number of copper coordinated systems are used to analyse the geometrical environment both at the metal and at the ligand ends. Except in special cases, the geometry exhibited by a coordinated system is often distorted. The aim of the present study is to get a quantitative idea of the range and dispersions of the various geometric parameters as well as the distortions from ideal geometrical situations.

Copper(II) has a  $3d^9$  outer electronic configuration and can form complexes of different geometries. The range of stereochemistries which have now been characterised for copper(II) and the factors which influence them have been summarised by Hathaway and Billing (1970). The major geometries that copper(II) takes up are octahedral (OCT) and square pyramidal (PY) and to a smaller extent square planar

\* For correspondence

(PL) and trigonal bipyramidal (TBP). On account of the close similarity between metal coordination and hydrogen bonding in so far as the ligand end is concerned, the formulation of parameters and the method of analysis employed in the present study closely follows that used in earlier studies from this group on hydrogen bonds (Ramachandran and Ramakrishnan 1967; Ramakrishnan and Prasad 1971; Mitra and Ramakrishnan 1977). The parameters at the metal end are of course very different.

## 2. Definition of parameters

The parameters that are used in the present study can be broadly classified as occurring at the metal end, associated with the geometry of coordination, or at the ligand end, associated with the lone pair orbitals of the ligand. The chief and most important parameter is the coordination bond length designated by  $l$ . This, in fact, can be taken to be associated with both ends, but for the present analysis it is grouped with metal end parameters.

The basis for defining the parameters at the ligand end is the same as that employed in the hydrogen bond studies done earlier in this group. There are three angular parameters  $\xi$ ,  $\zeta$  and  $\theta$  at the ligand end, and these involve the direction of the lone pair orbitals at the ligand atom. When there are two lone pair orbitals at the ligand atom the choice of associated orbital is made using the same criteria as in earlier hydrogen bond studies. Depending on the type of the ligand, a ligand plane is defined. The definition of the ligand plane in the various cases is given in table 1. While in (a) to (d) the lone pair orbitals are fixed in the ligand plane, for (e), where the nitrogen atom of the terminal amino group is the ligand atom, lone pair orbital is fixed

**Table 1.** The different ligand groups used and the relevance of the parameters at the ligand end, along with the number of examples used for each type of ligand.

Type	Ligand	Relevancy parameters			Number of examples used	Definition of ligand plane
		$\xi$	$\zeta$	$\theta$		
(a)	$\begin{array}{c} X \\ \diagdown \\ C=O \\ \diagup \\ Y \end{array}$	yes	yes	yes	101	Plane passing through C and O and fitting best with X and Y
(b)	$\begin{array}{c} X \\ \diagdown \\ O \\ \diagup \\ Y \end{array}$	yes	yes	yes	24	Plane containing lone pair orbitals (i.e., perpendicular to the plane XOY)
(c)	$\begin{array}{c} C & & N \\ & \diagdown & / \\ & C & \\ &    & \\ & O & \end{array}$	yes	yes	yes	9	Plane fitting best with the peptide group
(d)	$\begin{array}{c} C & & C \\ & \diagdown & / \\ & N & \end{array}$	yes	yes	yes	124	Plane CNC
(e)	$\begin{array}{c} H & & C \\ & \diagdown & / \\ & N & \\ & / & \\ H & & \end{array}$	no	no	yes	32	—

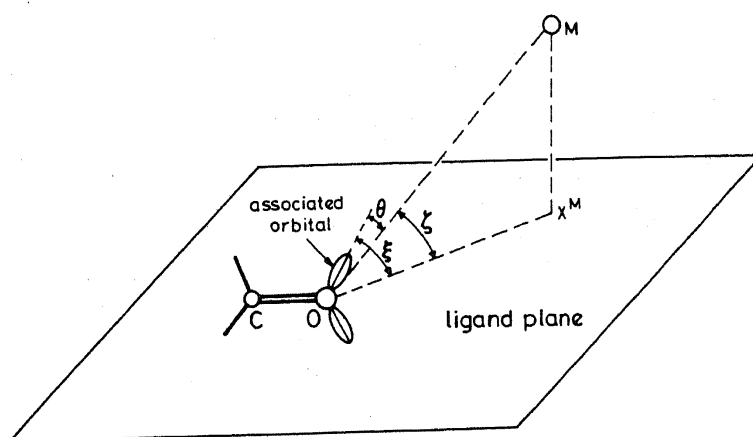


Figure 1. The parameters  $\xi$ ,  $\zeta$  and  $\theta$  at the ligand end. The figure corresponds to case (a) of table 1. M – metal atom (Cu);  $X^M$  – projection of metal-ligand direction onto the ligand plane. The orbital associated with the coordination bond is also shown.

tetrahedrally with respect to the three bonds meeting at the nitrogen atom, using the best-fit method.

The parameters  $\xi$ ,  $\zeta$  and  $\theta$ , as in the case of hydrogen bonds, are indicative of the spatial orientation of the  $M \dots L$  direction (M standing for the metal atom and L, the ligand atom) with the associated lone pair orbital. The parameter  $\xi$ , gives the angle between the associated lone pair orbital and the projection of the  $M \dots L$  direction on to the ligand plane,  $\zeta$ , the elevation of this direction from the ligand plane, and  $\theta$ , the geometrical angle between the  $M \dots L$  direction and the lone pair orbital. Figure 1 shows a schematic diagram of these parameters.

The relevance of the parameters and the number of examples of each type used in the various cases are given in table 1. Only nitrogen and oxygen ligand atoms are used in this study as the number of examples involving other atoms such as halogens, sulphur etc., is too small to be subjected to any meaningful analysis.

At the metal end, apart from the parameter  $l$  (coordination bond length), the other significant parameter is the coordination bond angle, and there are two kinds of these as described below.

In the octahedral arrangement, six ligand atoms surround the metal atom. By designating the axial atoms collectively as A and the four equatorial atoms collectively as E, it is possible to define the following parameters.

In the OCT geometry there are  ${}^6C_2$  (15) possible angles. These fall into three categories,  $A\hat{M}A$ ,  $A\hat{M}E$  and  $E\hat{M}E$ . This parameter is represented by  $\tau$  and the three subgroups are denoted by  $\tau_{AA}$ ,  $\tau_{AE}$  and  $\tau_{EE}$ . Among these  $\tau_{AA}$  is always around  $180^\circ$  and  $\tau_{AE}$  around  $90^\circ$ .  $\tau_{EE}$  however has different ranges of occurrence depending upon the coordination geometry.

For the ideal geometry (of OCT, PY and PL), the four equatorial atoms are coplanar and the line joining the two axial atoms passes through the metal atom and is also perpendicular to this plane. There are, however, distortions in any actual situation. A number of parameters have been defined to describe these distortions of the equatorial square and their values obtained (for details, see Geetha 1989). However only one parameter  $\delta_M$  is included in this paper. This gives the deviation of the metal atom from the plane which fits best with the four equatorial atoms (BP).

It can be seen that the parameter  $\tau_{AA}$  becomes irrelevant in the case of PY geometry

**Table 2.** Relevant parameters at the metal end for different geometries.

Parameter	OCT	PY	PL	TBP
$l$	yes	yes	yes	yes
$\tau_{AA}$	yes	no	no	yes
$\tau_{EE}$	yes	yes	yes	yes
$\tau_{AE}$	yes	yes	no	yes
$\delta_M$	yes	yes	yes	yes

as there is only one axial atom. Similarly any parameter connected with axial atoms becomes meaningless for PL geometry.

A summary of the relevant parameters at the metal end for different geometries is given in table 2. It must be mentioned that the coordination bond length ( $l$ ) and the coordination bond angle ( $\tau$ ) are the two parameters of great significance in energy calculations. The other parameters collectively serve the purpose of obtaining the proper coordination. These can prove to be very useful in computer modelling wherein the positions of the prospective ligand atoms can be checked for the suitability of coordination and the metal atom fixed in an appropriate manner (Geetha 1989).

The analysis has been carried out with data from seventy-five copper(II) complexes, comprising twenty-nine OCT, twenty-five PY, ten PL and eleven TBP geometries. A total of 370 coordination bonds has been used for this analysis. The structures, geometry, and number of bonds used in each as well as the citation details are given in table 3.

### 3. Method of analysis

The parameters, at the metal and the ligand ends as defined earlier, have been evaluated using the basic crystal structure data, viz. the coordinates of atoms involved in the metal coordinate system. The values have been sorted out and grouped under suitable intervals and the distributions are studied by plotting histograms. This is a commonly used type of parameter analysis and has been used by different workers for similar problems (Einsphar and Bugg 1980, 1981; Chiari and Ferraris 1982; Taylor *et al* 1983, 1984; Baker and Hubbard 1984; Yu *et al* 1985).

The first step in calculating the parameters at the metal end is to identify the axial atoms. While there is no difficulty in the cases of PY and TBP, there is some ambiguity for OCT coordination. In an ideal situation, the equatorial and axial ligand atoms are not uniquely defined and one can have three possible combinations. However, it is well-known that due to the Jahn-Teller effect, the symmetry is tetragonally distorted and thus there is a certain elongation of bonds in two diametrically opposite directions leading to their being defined as axial positions. We have taken the two atoms farthest away from the metal to be the axial atoms. However, we find that, interestingly, in all cases the angle subtended, by the two atoms so chosen, at the metal lies in the vicinity of  $180^\circ$ , thereby confirming their diametrically opposite disposition. In fact, this aspect gets further support from the distribution of bond lengths (cf. figure 2b).

**Table 3.** The ligand molecules, geometry of coordination and the citation details of the structures used in the present analysis.

Ligand molecule	Geometry of coordination	References
L-Leu-L-Tyr	PY	Van der Helm <i>et al</i> (1975)
Gly-Gly 2W	PY	Kistenmacher and Szalda (1975)
Bis(N-acetyl-Gly) 2W	OCT	Marcotrigiano <i>et al</i> (1976)
Bis(N-acetyl-Gly) 2W	OCT	Udupa and Krebs (1978)
Gly-L-Tyr 2W	PY	Mosset and Bonnet (1977)
bpy Gly-Cl	PY	Neitzel and Desiderato (1975)
Bis(2,3-di me py) 2Cl & 2Br	PL	Stahlin and Oswald (1971)
Imino diacetate 2W	OCT	Podder <i>et al</i> (1979)
L-Asp bpy W	PY	Antolini <i>et al</i> (1983)
Bis( $\delta$ -N-hydro-L-Orn) 2Cl	OCT	Stephens <i>et al</i> (1977)
L-Asp im	PY	Antolini <i>et al</i> (1982)
Bis(apa) 2W 2C104	OCT	Mosset <i>et al</i> (1976)
Butane di sulphonate-1, 4 4W	OCT	Charbonnier <i>et al</i> (1977)
Bis(2-amino-2-me-1-propanol)	PL	Muhonen (1981)
Gly-L-Met	PY	Bear and Freeman (1976)
L-Met-Gly	PY	Dehand <i>et al</i> (1979)
Py-2,6 dicarboxylate	OCT	Sarchet and Loiseleur (1973)
Bis(6-aminohexanoate)	OCT	Sjoberg <i>et al</i> (1973)
Gly-Gly 9-me-adenine 4W	PY	Kistenmacher <i>et al</i> (1976)
Bis(tcp) di im	OCT	Wong <i>et al</i> (1976)
Di aquo bis(salicylate)	PY	Jagner <i>et al</i> (1976)
$\alpha$ - $\beta$ -didehydro Gly-Gly-His W	PL	Meester and Hodgson (1978)
Bis(bpy) peroxy 2SO4	PY	Harrison and Hathaway (1980)
Bis(bpy) I	TBP	Hathaway and Murphy (1980)
Bis(bpy) Br	TBP	Hathaway and Murphy (1980)
Gly-Gly cytosine	PL	Kistenmacher <i>et al</i> (1975)
Bis(2-picoyl-phenyl ketonate)	PL	Sieler <i>et al</i> (1976)
(Salen) tu	PL	Ferrari <i>et al</i> (1976)
(Salof) tu	PL	Ferrari <i>et al</i> (1976)
Bis(L-Leu)	OCT	Fawcett <i>et al</i> (1979)
Bis(D, L-2-amino butyrate)	OCT	Fawcett <i>et al</i> (1979)
Gly-L-His-Gly	OCT	Meester and Hodgson (1977)
Bis(L-Asp)	OCT	Stephens <i>et al</i> (1975)
Bis(L-Met)	OCT	Ou <i>et al</i> (1978)
2,9-dime, phen Gly-Gly	PY	Simmons <i>et al</i> (1978)
L-Val-L-Tyr 4W	PY	Amirthalingam and Muralidharan (1976)
Nitrilo triacetate W	OCT	Whitlow (1973)
Bis(py-2-acetate) 2W	OCT	Faure and Loiseleur (1975)
Bis(dap) ClO4	OCT	West <i>et al</i> (1980)
Bis(propionate) 0, 5 dioxane	OCT	Borel and Leclaire (1976b)
Bis(propionate) $\beta$ -picoline	OCT	Borel and Leclaire (1976a)
Bis( $\beta$ -ala) 4W	OCT	Mitsui <i>et al</i> (1976)
Gly-Gly phen 3W	PY	Lim <i>et al</i> (1976)
Tetra- $\mu$ -N-ac-Gly 2W	OCT	Udupa and Krebs (1979)
Gly-Gly dmh	OCT	Marzilli <i>et al</i> (1979)
bea bpy NO3 2W	PY	Druhan and Hathaway (1979)
bea phen NO3	PY	Druhan and Hathaway (1979)
Aqua bis (LT)	PY	Lanfredi <i>et al</i> (1979)
Tetra aqua $\mu$ -9-me purine SO4	OCT	Sletten and Valand (1979)
Aqua phen oxalato W	PY	Fabretti <i>et al</i> (1985)

(Continued)

Table 3. (Continued)

Ligand molecule	Geometry of coordination	References
Bis(2-ethyl amino py 1-oxide)	PL	Knuuttila and Knuuttila (1986)
edp W	PY	Chapman <i>et al</i> (1981)
Bis(phen) Cl	TBP	Boys <i>et al</i> (1981)
O-phthalato bis (py)	PY	Cingi <i>et al</i> (1981)
bpy ida	PY	Nardin <i>et al</i> (1980)
Bis(bpy)	PY	Nardin <i>et al</i> (1980)
Bis(pydca)	TBP	Nardin <i>et al</i> (1980)
Hexakis(im) NO <sub>3</sub>	OCT	McFadden <i>et al</i> (1975)
Tris(phen)	OCT	Anderson (1973)
Ammine bis(bpy) BF <sub>4</sub>	TBP	Stephens (1972)
Bis(bpy) NCS	TBP	Tyagi and Hathaway (1981)
Bis(bpy) Cl	TBP	Stephens and Tucker (1973)
Bis(phen) CN	TBP	Anderson (1975)
Aqua bpy di thio di propionate	PY	Thich <i>et al</i> (1976)
Bis(bpy)	TBP	Kaiser <i>et al</i> (1974)
Tris (bpy) ClO <sub>4</sub>	OCT	Anderson (1972)
Tris (1,2di me im) 2 Cl	TBP	Huq and Skapski (1971)

## Abbreviations used:

apa	diamino-2, 3-propionic acid
tcp	2,4,6-trichloro phenolate
dap	2-dime amino pyridine-1-oxide
pydca	pyridine-2,6-dicarboxylate
bea	bis(2-amino ethyl) amine
edp	N,N'-ethylene di 2 pyridine carboxamide
LT	L-(+) threo-2-amino-1-phenyl-1, 3-propanediolato-N,O
salen	N,N'-ethylene bis(salicylaldimine)
salof	N,N'-o-phenylene bis(salicylaldimine)
ida	imino diacetate
dmh	7,9 di methyl hypoxanthine
bpy	2-2' bi pyridine
phen	1,10-phenanthroline

A computer program MCORD written in FORTRAN has been used to select the axial and equatorial atoms, fix the lone pair orbitals and also compute the various parameters mentioned above using the crystallographic coordinates of the involved atoms or groups as input.

For the present study the information regarding the atoms that are bonded to the metal, as well as the geometry of coordination have been directly taken from the respective crystal structure studies as reported therein. No further attempt has been made to find out whether there are any other atoms in the neighbourhood of the metal at bonding distances.

#### 4. Results and discussion

##### 4.1 Coordination bond length (*l*)

The parameter *l*, is found to vary from 1.8 to 3.0 Å in the cases studied. The distribution of values is shown in figure 2a as a histogram which shows a prominent peak between

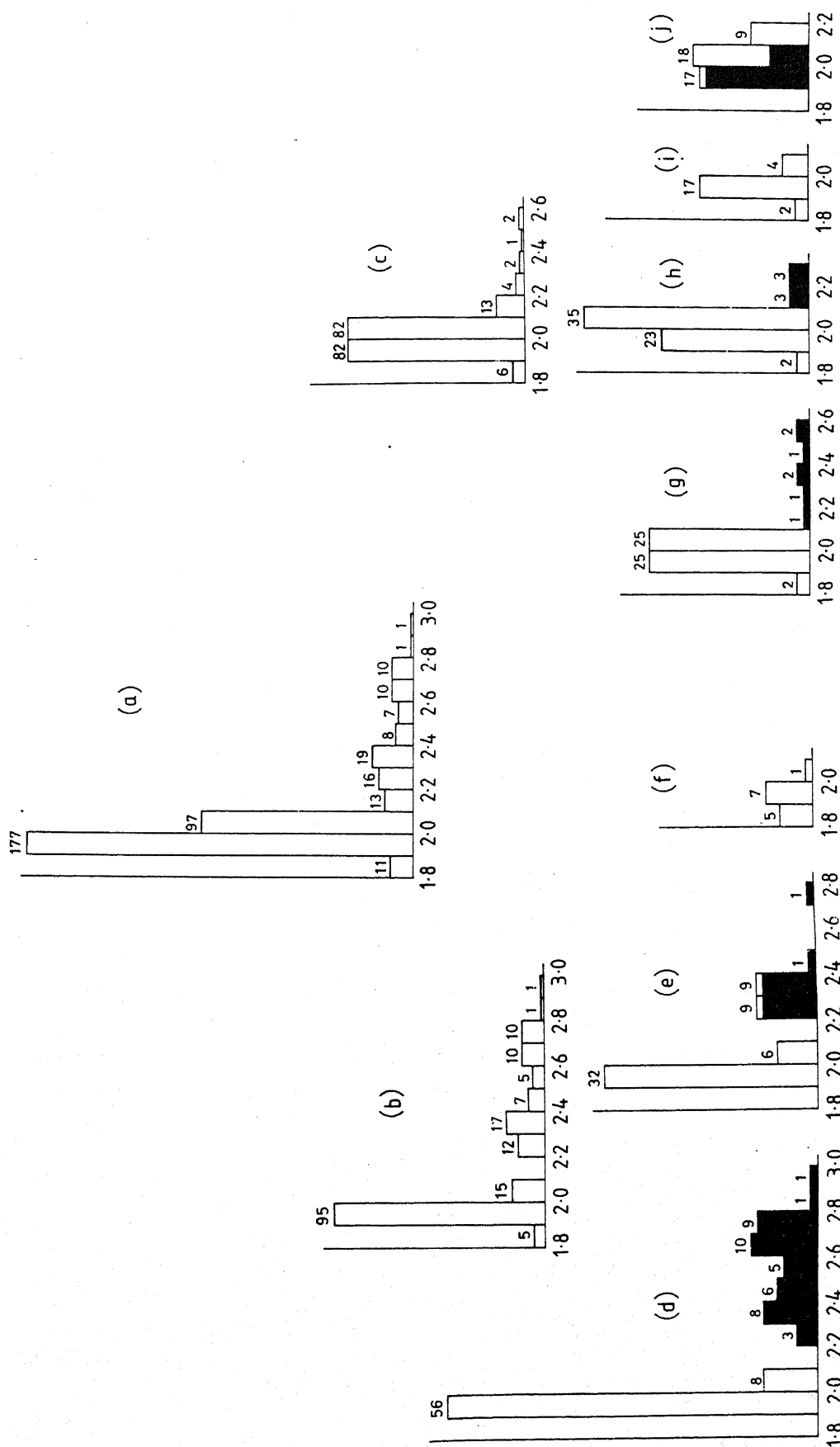


Figure 2. Histograms showing the distributions of the parameter  $l$  (Å). (a) General case; (b) oxygen ligand atom; (c) nitrogen ligand atom; (d) to (f) oxygen ligand atom in OCT, PY and PL geometries respectively; (g) to (i) nitrogen ligand atom in OCT, PY, PL and TBP geometries respectively. ■ = axial bonds.

1.9 and 2.0 Å. In fact 47.8% of the values lie in this range. The distribution falls very steeply on the lower value side. On the higher side, however, there is a two-step fall followed by a plateau.

In order to look at the variation in more depth, the distribution of this parameter corresponding to the two ligand atoms (O and N) as well as for different coordination geometries are drawn in figures 2b–2j.

The distribution for the oxygen ligand case (figure 2b) shows an interesting aspect. No values fall between 2.1 and 2.2 Å, thereby producing two regions. The first region shows a pronounced peak between 1.9 and 2.0 Å (similar to the one shown in figure 2a) and there is a near even distribution between 2.2 and 2.8 Å in the second region with a small peak between 2.3 and 2.4 Å.

This same trend is also exhibited in the sub-distributions corresponding to the OCT and PY cases (figure 2d and 2e) and is absent in the PL case (figure 2f).

Further examination of the values show that all the values between 2.2 and 3.0 Å (63) belong to axial positions of either OCT or PY geometry and none of the examples in the range 1.8–2.1 Å correspond to axial orientation. In a way this is to be expected since the identification of axial bonds has been made making use of the length, in the OCT geometry. What makes this interesting is that there is a small but definite gap separating the range of axial and equatorial lengths. The shortest axial bond is longer than the longest equatorial bond. The fact that this aspect is reflected in the case of PY geometry too is an indirect justification for choosing the two longest bonds as axial in the case of OCT geometry.

Figure 2f which gives the distribution for PL geometry shows a range of 1.8–2.1 Å with a peak between 1.9 and 2.0 Å. That there are no examples with lengths greater than 2.2 Å is to be expected since this geometry does not have any axial bond. It can be observed that all the five examples between 1.8 and 1.9 Å, shown in figure 2b, do have this coordination. Thus it can be deduced that in this coordination there is a tendency for the bonds to be short.

An analysis similar to the above can be made using the histograms shown in figure 2c and figures 2g–2j which correspond to examples having nitrogen as the ligand atom. The distribution shows a broad peak between 1.9 and 2.1 Å and falls off sharply on either side. This trend is equally well reflected for the OCT geometry (figure 2g) and to a lesser extent TBP (figure 2j). The peak value lies between 1.9 and 2.0 Å for PL and between 2.0 and 2.1 Å for PY geometries.

Unlike the case of oxygen ligand atoms, there are no two well-separated regions in these cases. In order to know whether there is any dependency of the range on the position of the ligand (axial or equatorial), the individual examples were looked into. The distribution of the length for the axial cases are shown as shaded regions in the histograms 2g, 2h and 2j. The lengths always tend to be on the higher side in the case of OCT and PY geometries (figures 2g and 2h). Thus the trend is similar to the one observed with the oxygen ligand atom and described earlier.

The distribution for TBP geometry (figure 2j), however, presents a very different and interesting situation. Almost all the examples in the range 1.9–2.0 Å belong to the axial orientation and this length does not go beyond 2.1 Å. This means, that unlike the cases of OCT and PY coordination, the axial bond is always shorter than the equatorial bond. In fact, this aspect was checked in the individual cases and found to be true.

The ranges for bond lengths observed in the different cases are collected and given in table 4 along with the average values and their standard deviations.



**Table 4.** Ranges, averages (Av) and standard deviations (SD) (in Å) for coordination bond lengths (*l*) in different geometries, and for different dispositions of the ligand atoms.

Geometry		O <sub>Eq</sub>	O <sub>Ax</sub>	N <sub>Eq</sub>	N <sub>Ax</sub>
OCT	Range	1.9–2.1	2.2–3.0	1.8–2.1	2.1–2.6
	Av	1.97	2.55	1.99	2.38
	SD	0.03	0.19	0.04	0.16
PY	Range	1.9–2.4	2.2–2.8	1.8–2.1	2.1–2.3
	Av	1.98	2.34	1.99	2.21
	SD	0.08	0.13	0.05	0.06
PL	Range	1.8–2.1		1.8–2.1	
	Av	1.91		1.96	
	SD	0.03		0.04	
TBP	Range			1.9–2.2	1.9–2.1
	Av			2.09	1.99
	SD			0.04	0.01

#### 4.2 Coordination bond angle ( $\tau$ )

As mentioned in an earlier section, there can be three types of angles,  $\tau_{AA}$ ,  $\tau_{AE}$  and  $\tau_{EE}$ , depending upon the ligand positions. It is apparent that the values of  $\tau_{AA}$  must be distributed around  $180^\circ$  and those of  $\tau_{AE}$  around  $90^\circ$ . The value of  $\tau_{EE}$  however can have a double distribution, one around  $90^\circ$  and another around  $180^\circ$  in the case of OCT, PY and PL, and  $120^\circ$  for TBP. The ranges, averages and standard deviations of the angles for different geometries are given in table 5, and the distributions in figures 3a–3f.

The distribution for  $\tau_{AA}$  is shown in figure 3a. There is a predominant peak between  $170$  and  $180^\circ$ . However, the values can be as low as  $130^\circ$ , though the number of values between  $130$  and  $170^\circ$  is only eight. This parameter is applicable only to OCT and TBP geometries. In figure 3a, the distribution for TBP is shown as hatched and all the 11 examples lie between  $170$  and  $180^\circ$ . Thus the tendency of the AMA direction to deviate from collinearity is less for TBP than for OCT coordination. In a semi-quantitative way the average and standard deviation of this parameter for the two cases reflect this aspect (table 5).

The distribution of the values which lie around  $90^\circ$  is shown in figure 3b–3e, with the distribution for  $\tau_{AE}$  being shaded. In all the cases, the peak of the distribution is between  $85$  and  $95^\circ$ . However, in the case of OCT geometry, there are some examples with values as low as  $45^\circ$  and as high as  $135^\circ$ . But their number is small compared to the peak value. The same trend is observed in PY also and the distribution is more skewed towards the higher side of  $90^\circ$ . In the case of TBP, there are no examples outside the range  $75$ – $105^\circ$  for  $\tau_{AE}$  (figure 3e).

Since the angles around  $90^\circ$  can have contributions from both  $\tau_{AE}$  and  $\tau_{EE}$ , it is worthwhile to examine which of these will have a greater spread (this is applicable to OCT and PY cases, since  $\tau_{AE}$  is not relevant to PL and the value of  $\tau_{EE}$  will be distributed around  $120^\circ$  for TBP). From the shaded region shown in figure 3b and 3c, it is clear that the spread arises from  $\tau_{AE}$ . This spread is more in the case of OCT than PY. In the latter distribution, there is an isolated example between  $45$  and  $55^\circ$  as well

**Table 5.** Ranges, averages (Av) and standard deviations (SD) (in degrees) for coordination bond angles ( $\tau$ ) in different geometries.

Geometry		$\tau_{AA}$	$\tau_{AE}$	$\tau_{EE}$
OCT	Range	130-180	45-130	75-105
	Av	171.1	90.2	89.9
	SD	13.9	11.8	5.0
PY	Range		75-115	75-115
	Av		95.7	90.3
	SD		8.5	7.5
PL	Range			75-105
	Av			90.2
	SD			4.7
TBP	Range	170-160	75-105	95-145
	Av	175.9	89.9	119.8
	SD	1.2	6.7	11.9

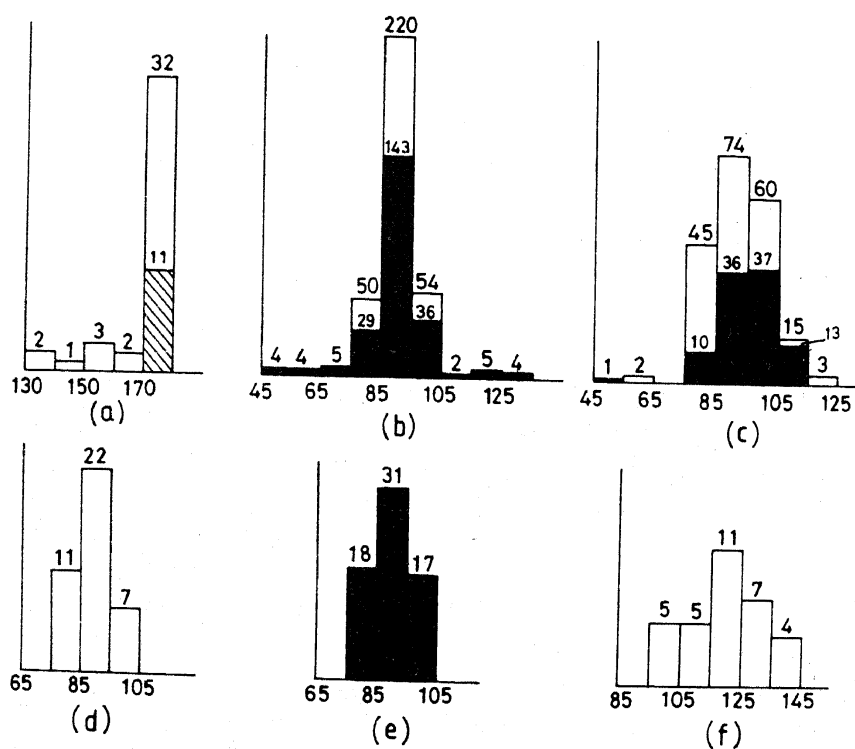


**Figure 3.** Histograms showing the distributions of the parameter  $\tau$  ( $^{\circ}$ ); (a)  $\square = \tau_{AA}$  for OCT,  $\boxtimes = \tau_{AA}$  for TBP, (b)  $\blacksquare = \tau_{AE}$  for OCT,  $\square = \tau_{EE}$  for OCT, (c)  $\blacksquare = \tau_{AE}$  for PY,  $\square = \tau_{EE}$  for PY (d)  $\tau_{EE}$  for PL, (e)  $\tau_{AE}$  for TBP, and (f)  $\tau_{EE}$  for TBP.

as three examples between 115 and 125 $^{\circ}$ . Actually, three of these four occur in the compound L-valine-L-tyrosine copper(II). 4H<sub>2</sub>O (Amirthalingam and Muralidharan 1976). In view of the fact that there are no examples between 55 and 75 $^{\circ}$ , this can be treated as an exception.

The distribution of  $\tau_{EE}$  shows a more uniform pattern in OCT, PY and PL

geometries. The range is 75–105° for OCT, PL and 75–115° for PY and hence for practical purposes the range can be taken as 75–105°. There are two examples between 55 and 65° for PY geometry, with no examples between 65 and 75° and 35 examples between 75 and 85°. Therefore these two examples can be treated as exceptions.

In the case of TBP,  $\tau_{AE}$  ranges from 75–105° and  $\tau_{EE}$  has a broader range between 95 and 145°. From table 5, it can be seen that in the OCT case the standard deviation is smallest for  $\tau_{EE}$  and increases for  $\tau_{AE}$  and  $\tau_{AA}$ . It is interesting to note that this trend is exactly opposite to that for the TBP case.  $\tau_{AE}$  shows greater clustering, compared to  $\tau_{EE}$  for TBP geometry.

#### 4.3 Deviation of the metal from the best plane ( $\delta_M$ )

The general distribution for this parameter is given in figure 4a. The distributions of the parameter for OCT, PY, PL and TBP are shown in figures 4b–4e. It can be seen that the range is very narrow (0–0.05 Å) for TBP, and largest (0–0.4 Å) for PY geometry. The range for OCT is 0–0.25 Å and 0–0.1 Å for PL geometry.

The average value of the deviation for TBP is 0.006 Å and the standard deviation is 0.003 Å, indicating that the metal is nearly in the plane of the equatorial atoms. The corresponding values for PL and OCT cases are 0.04 Å ( $\sigma = 0.02$ ) and 0.08 Å ( $\sigma = 0.07$ ) respectively indicating that the metal is more deviated from the plane in these cases. The largest value however is found for the PY case with an average of 0.19 Å and standard deviation of 0.09 Å. There are two examples between 0.35 and 0.4 Å, which are very large as compared to others.

That the deviation of the metal atom is largest for the PY case can be understood since in this case the metal atom is subjected to an asymmetric pull by the lone axial atom. In fact, an interesting observation made in the present study is that the shift of the metal atom in all the PY cases is on the same side of the best plane as the axial ligand. In the OCT and TBP cases, the deviations, as expected, are smaller than

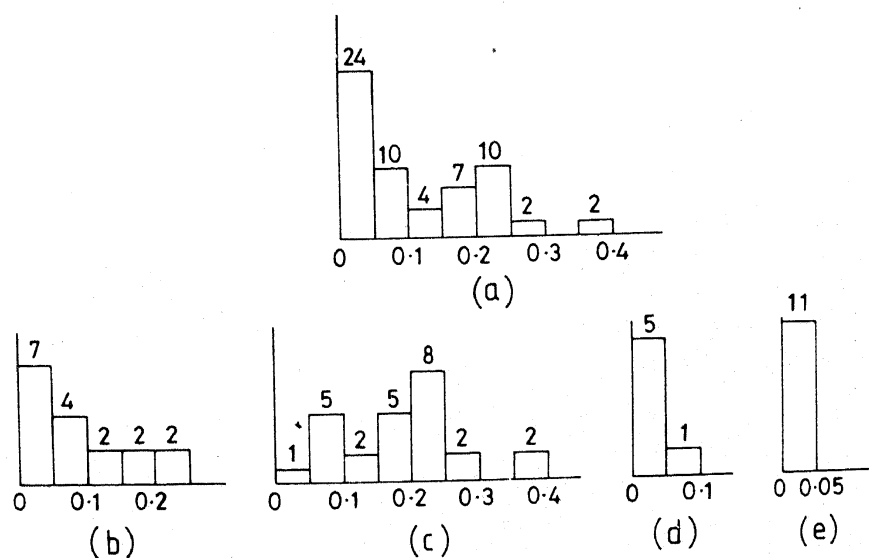


Figure 4. Histograms showing the distributions of the parameter  $\delta_M$  (Å). (a) General; (b) OCT; (c) PY; (d) PL; and (e) TBP geometries.

for PY in view of the symmetric pull by the two axial atoms. In the case of PL, the metal is not subjected to any axial pull.

The three parameters discussed so far involve the metal atom. In addition, four other parameters pertaining to virtual bond lengths and virtual bond angles connected with the equatorial square have also been defined, and the data collected and analysed. The details of these in the form of histograms are available elsewhere (Geetha 1989). The results indicate that the ideal square can be distorted up to 0.4 Å for its side and 10° for its angle. The deviation of the equatorial atoms from the best plane ranges from 0 to 0.25 Å (Geetha 1989).

#### 4.4 Ligand end parameters

The distribution for the three parameters defined at the ligand end, viz.  $\theta$ ,  $\zeta$  and  $\xi$ , are shown in figures 5a, 5d and 5g respectively. The individual distributions for the oxygen ligand atoms are shown in figure 5b, 5e and 5h and the corresponding histograms for the nitrogen ligand atoms are shown in figures 5c, 5f and 5i respectively.

The general distribution for the three parameters have the common feature in that the peak occurs for the range 0–10° and a considerable percentage of values lies in this range (59.6, 81.4, 71.7% respectively). The range for these parameters can be taken to be 0–60°, with a few examples (1%) lying outside this range. The distribution for  $\theta$  falls off more gradually than for the other two parameters.

From the distributions of the three parameters for oxygen and nitrogen ligand atoms, we observe (i) the spread of values is larger in the case of oxygen than for nitrogen, (ii) the fall-off in the case of nitrogen is much steeper than for oxygen.

In order to compare the present situation with that existing in hydrogen bond cases, the corresponding distributions for  $\theta$ ,  $\zeta$  and  $\xi$  are shown in figures 5j, 5k and 5l respectively. These have been drawn using data from figures 10d, 5b and 7b of Mitra and Ramakrishnan (1977) for O–H...O bonds and the updated data of figures 13b, 5b and 8a of Ramakrishnan and Prasad (1971), obtained from Prasad (1972), for N–H...O bonds.

In the distribution for  $\theta$ , the peak is shifted to the right (20–30°) as compared to the present case (0–10°). The peak for  $\zeta$  is between 0 and 10° for the hydrogen bond case also. In the case of  $\xi$ , the peak is very broad (0–20°). Comparing the corresponding histograms for the coordination bonds, we observe that the range is broader and falls off more gradually in the hydrogen bond cases. Based upon this, it can be said that the M...L bond has a much stronger tendency to cling to the orbital with which it is associated. This can also be interpreted to mean that the direction of the coordination bond is more highly influenced by the lone pair orbitals than that of the hydrogen bond.

It was shown in the earlier studies on hydrogen bonds that the distribution of  $\xi$  was dependent on whether the acceptor oxygen atom is the recipient of one hydrogen bond or two. In addition there was a definite distinction in the distribution when the projection of the H...O direction falls in between orbitals as compared to the situation when it falls outside the orbitals. From the data given in table 9 of Mitra and Ramakrishnan (1977), it is clear that the peak which is between 0 and 10° for the two bond acceptor case (irrespective of the H...O projection position) as well as for the one-bond acceptor case, when the projection falls outside the orbitals, shifts to the range 20–30° when the projection falls between orbitals.

In order to find out whether a similar effect is observable in the present case, the

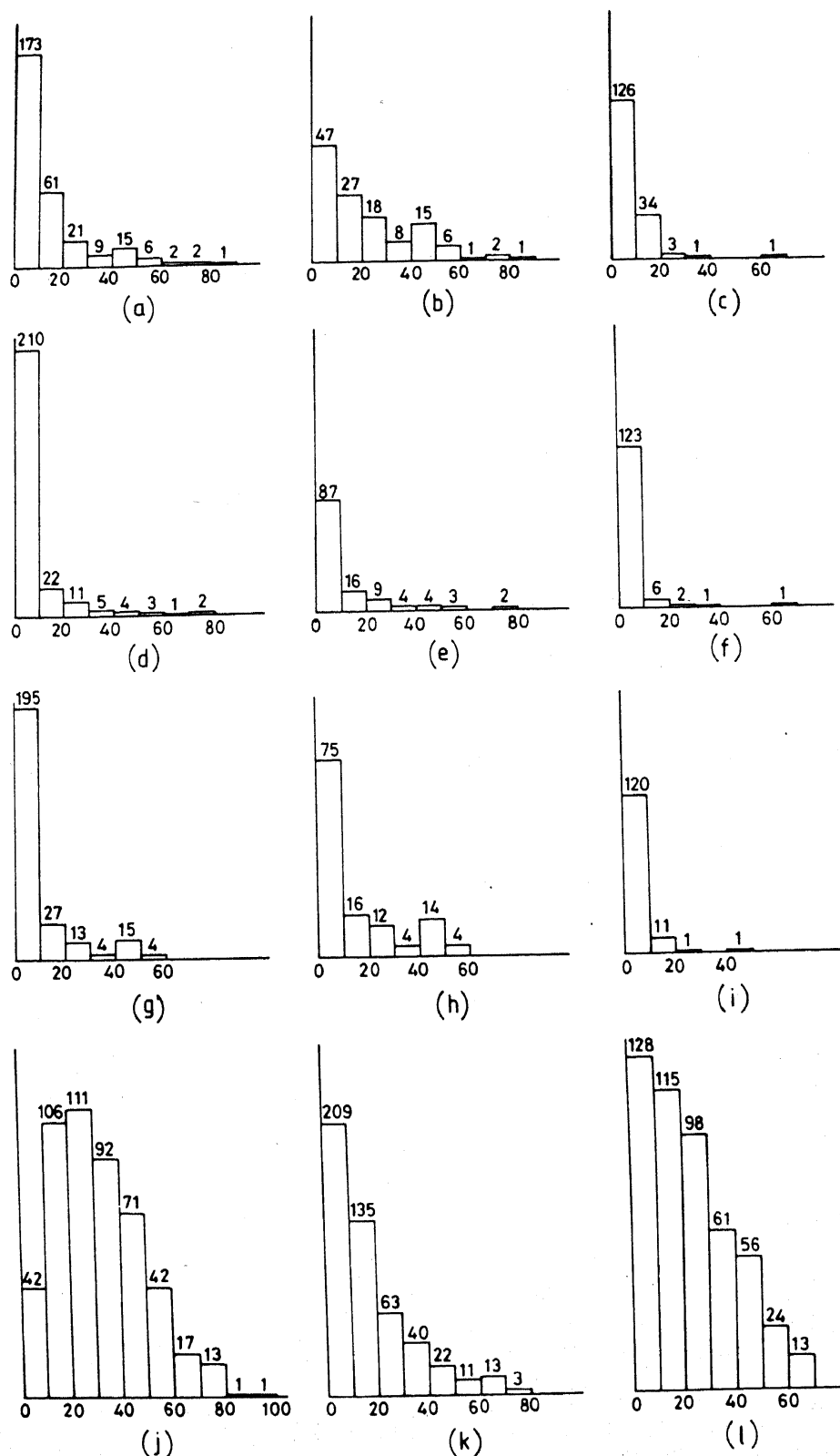


**Figure 5.** Histograms showing the distributions of the ligand end parameters: (a)–(c) distribution of  $\theta$ ; (d)–(f) distribution of  $\zeta$ ; and (g)–(i) distribution of  $\xi$ ; all in degrees. (a), (d) and (g) general; (b), (e) and (h) oxygen ligand atom; (c), (f) and (i) nitrogen ligand atom. The corresponding acceptor end parameters for hydrogen bonds are: (j) distribution of  $\theta$ ; (k) distribution of  $\zeta$ ; and (l) distribution of  $\xi$ .

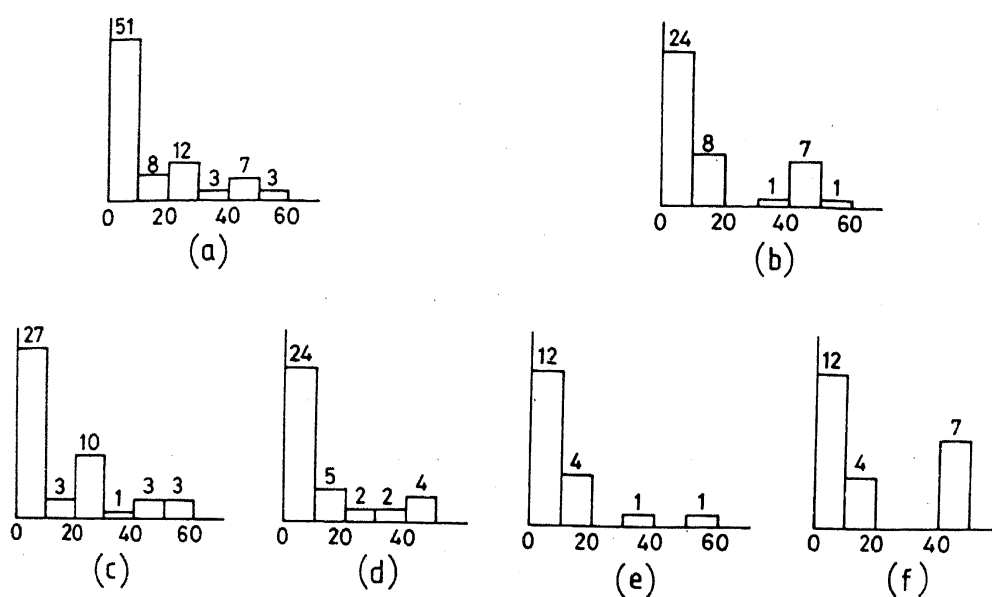


**Figure 6.** Histograms showing the distributions of  $\xi$  in different cases. (a) One-bond acceptor; (b) two-bond acceptor; and (c) one-bond acceptor, with the projection lying in-between the orbitals; (d) one-bond acceptor, with the projection lying outside the orbitals; (e) two-bond acceptor, with the projection lying in-between the orbitals; and (f) two-bond acceptor, with the projection lying outside the orbitals.

distributions of  $\xi$  under different situations are given in figures 6a–f. The histograms clearly indicate the absence of such an effect. In fact, the peak position lies between 0 and 10° in all the histograms. This shows that the influence of the other non-associated orbital on the bonding direction is far less and is also independent of whether the projection lies between the orbitals or outside the orbitals in the ligand plane.

### Acknowledgements

The authors would like to thank Dr N V Joshi for useful and interesting discussions. One of us (YSG) would like to thank the University Grants Commission for financial support.

### References

- Amirthalingam V and Muralidharan K V 1976 *Acta Cryst.* **B32** 3153
- Anderson O P 1972 *J. Chem. Soc., Dalton Trans.* 2597
- Anderson O P 1973 *J. Chem. Soc., Dalton Trans.* 1237
- Anderson O P 1975 *Inorg. Chem.* **14** 730
- Antolini L, Marcotrigiano G, Menabue L and Pellacini G E 1983 *Inorg. Chem.* **22** 141
- Antolini L, Marcotrigiano G, Menabue L, Pellacini G E and Saladini M 1982 *Inorg. Chem.* **21** 2263
- Baker E N and Hubbard R E 1984 *Prog. Biophys. Mol. Biol.* **44** 97
- Bear C A and Freeman H C 1976 *Acta Cryst.* **B32** 2534
- Borel P M M and Leclaire A 1976a *Acta Cryst.* **B32** 1273
- Borel P M M and Leclaire A 1976b *Acta Cryst.* **B32** 1275
- Boys D, Escobar C and Carrera S M 1981 *Acta Cryst.* **B37** 351
- Chapman R L, Stephens F S and Vagg R S 1981 *Acta Cryst.* **B37** 75

- Charbonnier P F, Faure R and Loiseleur H 1977 *Acta Cryst.* **B33** 3759  
Chiari G and Ferraris G 1982 *Acta Cryst.* **B38** 2331  
Cingi M B, Lanfredi A M M, Tiripicchio A and Camellini M T 1981 *Acta Cryst.* **B37** 2159  
Dehand J, Jordanov J, Keck F, Mosset A, Bonnet J J and Galy J 1979 *Inorg. Chem.* **18** 1543  
Druhan G and Hathaway B J 1979 *Acta Cryst.* **B35** 344  
Einsphar H and Bugg C E 1980 *Acta Cryst.* **B36** 264  
Einsphar H and Bugg C E 1981 *Acta Cryst.* **B37** 1044  
Fabretti A C, Franchini G and Zannini P 1985 *Inorg. Chim. Acta* **105** 187  
Faure P R and Loiseleur H 1975 *Acta Cryst.* **B31** 1472  
Fawcett T G, Ushay M, Rose J P, Lalancette R A, Potenza J A and Schugar H J 1979 *Inorg. Chem.* **18** 327  
Ferrari M B, Fava G G and Pellizi C 1976 *Acta Cryst.* **B32** 901  
Geetha Y S 1989 *Studies on geometrical aspects of metal coordination*, Ph D thesis, Indian Institute of Science, Bangalore  
Harrison W D and Hathaway B J 1980 *Acta Cryst.* **B36** 1069  
Hathaway B J and Billing D E 1970 *Coordination Chem. Rev.* **5** 143  
Hathaway B J and Murphy A 1980 *Acta Cryst.* **B36** 295  
Huq F and Skapski A C 1971 *J. Chem. Soc. A* 1927  
Jagner S, Hazell R G and Larsen K P 1976 *Acta Cryst.* **B32** 548  
Kaiser J, Brauer G, Schroder A F, Taylor I F and Rasmussen S E 1974 *J. Chem. Soc., Dalton Trans.* 1490  
Kistenmacher T J, Marzilli L G and Szalda D J 1976 *Acta Cryst.* **B32** 186  
Kistenmacher T J and Szalda D J 1975 *Acta Cryst.* **B31** 1659  
Kistenmacher T J, Szalda D J and Marzilli L G 1975 *Acta Cryst.* **B31** 2416  
Knuutila P and Knuutila H 1986 *Acta Cryst.* **C42** 989  
Lanfredi A M M, Tiripicchio A and Camellini M T 1979 *Acta Cryst.* **B35** 349  
Lim M C, Sinn E and Martin R B 1976 *Inorg. Chem.* **15** 807  
Marcotrigiano G, Pellacani G C, Battaglia L P and Corradi A B 1976 *Cryst. Struct. Commun.* **5** 923  
Marzilli L G, Wilkowski K, Chiang C C and Kistenmacher T J 1979 *J. Am. Chem. Soc.* **101** 7504  
McFadden D L, McPhail A T, Garner C D and Mabbs F E 1975 *J. Chem. Soc., Dalton Trans.* 263  
Meester P D and Hodgson D J 1977 *Acta Cryst.* **B33** 3505  
Meester P D and Hodgson D J 1978 *Inorg. Chem.* **17** 440  
Mittra J and Ramakrishnan C 1977 *Int. J. Pept. Protein Res.* **9** 27  
Mitsui Y, Iitaka Y and Sakaguchi H 1976 *Acta Cryst.* **B32** 1634  
Mosset P A and Bonnet J J 1977 *Acta Cryst.* **B33** 2807  
Mosset P A, Bonnet J J and Jeanin Y 1976 *Acta Cryst.* **B32** 591  
Muhonen H 1981 *Acta Cryst.* **B37** 951  
Nardin G, Randaccio L, Bonomo R P and Rizzarelli E 1980 *J. Chem. Soc., Dalton Trans.* 369  
Neitzel C J and Desiderato R 1975 *Cryst. Struct. Commun.* **4** 333  
Ou C C, Powers D A, Thich J A, Felthouse T R, Hendrickson D N, Potenza J A and Schugar H J 1978 *Inorg. Chem.* **17** 34  
Podder A, Dattagupta J K, Saha N N and Saengar W 1979 *Acta Cryst.* **B35** 53  
Prasad N 1972 *Theory of biopolymer conformations*, Ph D thesis, University of Madras  
Ramachandran G N and Ramakrishnan C 1967 *Fibrous proteins* (ed) W G Crewther (Australia: Butterworths) p.71  
Ramakrishnan C and Prasad N 1971 *Int. J. Protein. Res.* **3** 209  
Sarchet P C and Loiseleur H 1973 *Acta Cryst.* **B29** 1345  
Sieler V J, Kaiser J, Richter R and Schmidt W 1976 *Acta Cryst.* **B32** 452  
Simmons C J, Lundeen M and Seff K 1978 *Inorg. Chem.* **17** 1429  
Sjoberg B, Osterberg R and Soderquist R 1973 *Acta Cryst.* **B29** 1136  
Sletten E and Valand E 1979 *Acta Cryst.* **B35** 840  
Stahlin W and Oswald H R 1971 *Acta Cryst.* **B27** 1368  
Stephens F S 1972 *J. Chem. Soc., Dalton Trans.* 1350  
Stephens F S and Tucker P A 1973 *J. Chem. Soc., Dalton Trans.* 2293  
Stephens F S, Vagg R S and Williams P A 1975 *Acta Cryst.* **B31** 841  
Stephens F S, Vagg R S and Williams P A 1977 *Acta Cryst.* **B33** 438  
Taylor R, Kennard O and Verischel W 1983 *J. Am. Chem. Soc.* **105** 5761  
Taylor R, Kennard O and Verischel W 1984 *Acta Cryst.* **B40** 280  
Thich J A, Lalancette R A, Potenza J A and Schugar H J 1976 *Inorg. Chem.* **15** 2731  
Tyagi S and Hathaway B J 1981 *J. Chem. Soc., Dalton Trans.* 2029

- Udapa M R and Krebs B 1978 *Inorg. Chim. Acta* **31** 251  
Udapa M R and Krebs B 1979 *Inorg. Chim. Acta* **37** 1  
Van der Helm D, Ealick S E and Burks J E 1975 *Acta Cryst.* **B31** 1013  
West D X, Pavkovic S F and Brown J N 1980 *Acta Cryst.* **B36** 143  
Whitlow S H 1973 *Inorg. Chem.* **12** 2286  
Wong R Y, Palmer K J and Tomimatsu Y 1976 *Acta Cryst.* **B32** 567  
Yu H A, Karplus M and Hendrickson W A 1985 *Acta Cryst.* **B34** 191